Impact of Unit Commitment and RoCoF Constraints on Revenue Sufficiency in Decarbonising Wholesale Electricity Markets

Daniel Marshman*, Michael Brear

Department of Mechanical Engineering, The University of Melbourne, Parkville 3010, Australia

Brendan Ring

Market Reform, Melbourne, Australia

Abstract

This paper examines the impact of unit commitment (UC) and rate of change of frequency (RoCoF) constraints on the performance and revenue sufficiency of decarbonising wholesale electricity markets. Different environmental policy and cost inputs are first used to produce increasingly decarbonised fleets with large differences in the uptake of wind, solar and flexible plant by using generation expansion (GE) planning without either of these constraints. The performance of these fleets is then assessed with and without UC and RoCoF constraints in a conventional economic dispatch (ED) framework.

It is found that conventional GE planning tools without UC and RoCoF constraints should produce fleets that can transact via an efficient wholesale market if there is less than approximately 40% wind and 20% solar PV by annual generation. In this case, system average costs should match average prices, all generating units' internal rates of return should match the cost of capital used in the GE plan and costs to consumers should be minimised. However, the inclusion of UC, RoCoF and potentially other reliability and security considerations may be required in GE planning tools beyond these approximate limits of renewable generation, with greater deployment of flexible plant including energy storage not necessarily solving the observed problems.

1. Introduction

Many jurisdictions are encouraging investment in renewable generation sources, mainly wind and solar photovoltaics (PV) which collectively are termed variable renewable generation (VRG) [1]. As VRG capacity grows, it can become increasingly difficult to schedule other resources. Moreover, VRG does not typically provide ancillary services, such as reserves, inertia or voltage support, which are necessary for secure power system operation. Such operational considerations relate to system security and reliability and are also not normally included in generation expansion (GE) planning models due to their computational cost [2, 3].

Of course, pumped hydro energy storage (PHES) and battery storage can assist with the integration of VRG. Both of these technologies can operate very flexibly in terms of ramping capability and reserves provision [4]. However, batteries do not provide inertia.

Of course, true inertia is provided by rotating machines that are synchronously connected to the grid [5]. When a power imbalance occurs system inertia acts against the change in frequency. With more inertia, the rate of change of frequency (RoCoF) in a contingency event will be slower, giving more time for frequency control ancillary services to activate and arrest changes in the system frequency. With more energy being provided by non-synchronous generation, power systems may be exposed to higher RoCoF during contingencies, which may then result in further generator trips, under-frequency load-shedding, and other responses [6]. Reductions in levels of inertia have been observed in power systems in Australia [7, 8], Texas [9] and Ire-

*Corresponding author

land [10]. Recently some studies have investigated impacts of falling inertia levels on system security in the Australian National Electricity Market (NEM) [6, 11, 12] and internationally [13].

As hydro-thermal units only provide inertia when committed, limiting maximum potential RoCoF is directly linked with unit commitment (UC). Many studies have examined the impacts of VRG on UC decisions e.g. [13–17]. A further concern is the emerging recognition that the planning problem may need to consider flexibility adequacy in addition to capacity adequacy [2].

Indeed, several studies have examined how VRG influences the need to include UC constraints in planning models [14, 18–21]. Both Shortt et al. [14] and Jin et al. [20] compared the performance of fleets in models with and without UC constraints. While the latter found that UC constraints had only minor impacts on optimal expansion decisions, the former found that impacts could be significant, and were dependent upon several factors, including the system demand profile, the capacity of storage or nuclear generation, and of course the wind penetration. Palmintier & Webster [19] found that UC materially impacts the planning problem at about 20% wind energy, due to conflicting reliability and environmental targets. Again the system-specific dependency of this conclusion was noted.

Equivalent studies that consider solar PV are more limited. Chen et al. [21] did include solar and storage, but did not include integer UC decisions, instead using a linearised model for reasons of computational cost. Studies (e.g. [22, 23]) have nonetheless found that solar curtailment becomes significant at relatively low penetrations, indicating the value of further investigation.

The consequences of ignoring UC and security constraints in planning models can include higher total operating costs, emissions and VRG curtailment. These consequences may also impact the financial performance of all generation investments, since in liberalised electricity markets, investment and operational decisions are made by individual actors. VRG with low short-run marginal costs (SRMCs) can depress both electricity prices [24, 25] and generator revenues [26, 27]. But this should be a transient effect [27], as lower prices should signal that some capacity should exit, increasing average prices and returns to the capacity that remains [27, 28]. Indeed, Riesz & Gilmore [29] found that generators could recover their long-run costs in 100% renewable systems, assuming the market had adjusted to a least-cost equilibrium. This result rests on much earlier research [30–32] in electricity pricing. When investment and operational decisions are optimal - i.e. investors correctly anticipate future electricity demand, VRG availability, etc - prices set at the short-run marginal cost will allow generators to recover their investment and operating costs.

However, this result does not necessarily hold when non-convex constraints such as UC are included. In such cases, marginal spot prices may not always support the least-cost solution and some form of additional side-payment may be required for generators to recover their costs [33, 34]. Such interactions are historically minor, but with growth in VRG resulting in more severe ramps, lower minimum demand, and more frequent generator cycling [35], the potential for markets to send sub-optimal signals for both operational and investment decisions could grow. De Sisternes et al. [36] and Marshman et al. [28] have investigated revenue sufficiency for thermal generators with such non-convex UC constraints and thermal fleets which either remain fixed, or are optimised for each incremental level of VRG uptake. Both studies found that the impacts of the merit-order effect (with no thermal plant exit) on revenue sufficiency far outweigh that due to non-convex effects. However, the former study did not consider revenue sufficiency of VRG, while the latter did not include solar. Also, neither study systematically considered different levels of flexibility in the generation fleet, or the impacts of storage.

As such, this paper examines the conditions for which UC and RoCoF constraints materially impact revenue sufficiency for thermal, renewable and storage technologies participating in a decarbonising electricity market. In addition, the effect of various levels of a RoCoF constraint on generator financial performance is investigated. Implications for system planning are then discussed.

2. Method

2.1. Overview and Generating Fleets

In this work, the technical, financial and environmental performance of various generation fleets are first determined in a GE sub-model and then compared in operational sub-models with and without UC constraints. These are termed the Unit Commitment and Economic Dispatch (UC+ED) and

Economic Dispatch Only (ED-Only) sub-models, respectively. Input data is based on the Victorian region of the Australian NEM. The available technologies are

- coal,
- combined cycle gas turbines (CCGTs),
- open cycle gas turbines (OCGTs),
- nuclear,
- wind,
- solar PV,
- battery storage.

An overview of the modelling process is provided in Figure 1, and further details are given in our previous work, Marshman et al. [28].

Table 1 shows that fives types of fleets are considered, with each fleet also subjected to different environmental policies. Either a carbon price or a renewable energy certificate (REC) price - as used to achieve a renewable portfolio standard (RPS) - is applied to each fleet. These range from \$0/t to \$100/t as a carbon price and \$0/MWh to \$100/MWh as a REC price.

Cost inputs from either the 2012 or 2050 scenarios in the Bureau of Resources & Energy Economics (BREE) Australian Energy Technology Assessment (AETA) [37] datasets are also used. This primarily affects the costs of wind, solar and thermal plant, with the 2050 dataset making solar more favourable than wind. Whilst this dataset is now relatively old, these cost inputs only impact the modelled absolute costs in this paper and do not change the technical modelling or the arguments put forward.

Battery storage was not included in the AETA dataset, and hence its reference capital cost was sourced separately. Four of the fleets assume that energy storage has a capital cost of \$500/kWh, which is thought representative of current costs [38, 39]. However, the GE model does not build any storage at this cost. Therefore, the storage fleet uses \$250/kWh as a plausible future capital cost. Finally, nuclear was also disallowed in some cases to promote VRG.

The demand trace from the Victorian region of the NEM for 2017 is used, for which peak demand was 8.6 GW, and annual consumption was 43.4 TWh. The wind trace is from the summation of generation from Victorian wind generators (approximately 1.4 GW capacity in 2017), normalised by capacity. Because of limited utility scale solar in Victoria for that period, the solar trace is instead taken from the combined output of solar farms in New South Wales (approximately 250 MW capacity), again normalised by capacity. Capacity factors of the wind and solar traces are 32% and 25% respectively. The market price cap (MPC) was based on that of the NEM, \$14,000/MWh. Technology capital costs were annualised with a discount rate of 10%, as in the AETA [37], which can be considered the cost of capital.

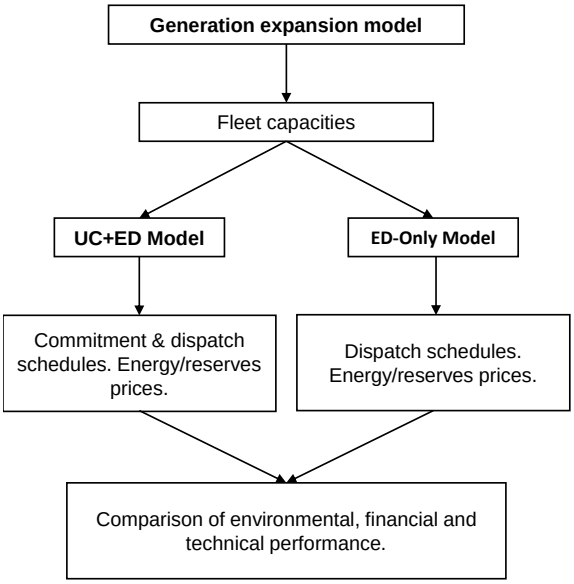

Figure 1: Method overview. Text in boldface denotes an optimisation model.

2.2. Generation Expansion Model Sub-Model

A capacity mix is first determined in a conventional GE sub-model without UC constraints and which minimizes the sum of:

- Annualized capital costs,
- Fixed operating & maintenance (FOM) costs,
- Variable operating & maintenance (VOM) costs,
- Fuel costs,
- Penalty costs on energy/reserves shortages,
- Emissions, due to a carbon price (if applicable),
- The *value* of renewable energy, at the REC price (if applicable).

The GE sub-model is run at hourly resolution for a one-year horizon and assumes that only new assets are built in each simulation. As UC constraints are not included, units can generate within their

Fleet Name	AETA Cost Inputs	Policy	Nuclear Available	Storage Capital Cost
Wind fleet	2012	RPS	Yes	\$500/kWh
Solar fleet [RPS]	2050	RPS	Yes	\$500/kWh
Solar fleet [CP]	2050	Carbon Price	No	\$500/kWh
Nuclear fleet	2012	Carbon Price	Yes	\$500/kWh
Storage fleet	2050	RPS	Yes	\$250/kWh

Table 1: Characteristics of the five fleets.

capacity and ramping constraints. Five types of reserve are included (primary raise/lower, secondary raise/lower, tertiary raise) with each given a requirement. Each technology is also given the ability to provide different combinations of these reserves. The full GE sub-model formulation is available in Marshman [40].

2.3. Commitment and Dispatch Decisions

Following determination of each fleet's capacity mix, two versions of a UC model are used to determine operational decisions. This model is based on a formulation presented by Palmintier et al. [41], in which generating units are grouped by technology type with all units in a cluster being identical. We first describe the UC+ED version.

2.3.1. UC+ED Sub-Model

Given the GE decisions, the UC+ED sub-model minimizes the total expected operational costs of delivering electricity, including policy costs and the costs of load load or insufficient reserves, and includes uncertainty in wind, solar and electricity demand.

The objective function is

$$C^{\mathrm{To}} = \sum_{sg} \pi_s \left(C^{\mathrm{Va}}_{sg} + C^{\mathrm{St}}_{sg} + C^{\mathrm{Ca}}_{sg} - C^{\mathrm{Re}}_{sg}\right) + \sum_{s} \pi_s C^{\mathrm{Un}}_{s}, \tag{1}$$

in which π_s is the probability of scenario s, with scenarios representing different VRG and load forecasts. The bracketed cost terms represent, respectively, the variable costs (i.e. fuel and VOM costs), start-up/shut-down costs, costs associated with the carbon price, and with the value of RECs produced, for each scenario s and generator g. The final term represents the costs associated with unserved energy and insufficient reserves.

These cost terms are defined as follows:

$$C^{\mathrm{Va}}_{sg} = \sum_{h} p_{shg} (3.6 c^{\mathrm{FC}}_{g} / \eta^{g}_{\mathrm{th}} + c^{\mathrm{VOM}}_{g}), \tag{2}$$

$$C^{\mathrm{St}}_{sg} = \sum_{h} \left(c^{\mathrm{U}}_{g} S^{\mathrm{U}}_{shg} + c^{\mathrm{D}}_{g} S^{\mathrm{D}}_{shg}\right) \quad g \in \mathcal{G}_D \setminus \mathcal{G}_S, \tag{3}$$

$$C^{\mathrm{Ca}}_{sg} = P^{\mathrm{Ca}} \mathrm{E}_g \sum_{h} p_{shg}, \tag{4}$$

$$C^{\mathrm{Re}}_{sg} = P^{\mathrm{Re}} \sum_{h} p_{shg} \quad g \in \mathcal{G}_R. \tag{5}$$

$$C^{\mathrm{Re}}_{sg} = 0 \quad g \notin \mathcal{G}_R, \tag{6}$$

$$C^{\mathrm{Un}}_{s} = P^{\mathrm{MPC}} \left[\sum_{h} u^{\mathrm{e}}_{sh} + \sum_{hr} u^{\mathrm{r}}_{shr}\right]. \tag{7}$$

In Eq. (2), the first term accounts for fuel costs due to power generation, p_{shg} in each period h, with η^{g}_{th} being the thermal efficiency of the technology g. The second term similarly accounts for VOM costs. Eq. (3) calculates the start-up costs as the product of unit start events S^{U}_{shg} in a period h, and the start-up cost c^{U}_{g} of a technology (and similarly for shut down costs). Eq. (4) determines the cost of carbon emissions at the carbon price P^{Ca} using a technology's emissions intensity E_g. For renewable generators, generation is valued at the REC price, P^{Re} (Eq. 5), with this term set to zero for non-renewable generators (Eq. 6). Finally, any unserved demand or insufficient reserve availability is charged at the MPC, P^{MPC} in Eq. (7).

The power generation plus raise reserve enablement of technology clusters is of course limited by the committed capacity, e.g.

$$p_{shg} + \sum_{r \in \{\bar{\mathrm{p}}, \bar{\mathrm{s}}, \bar{\mathrm{t}}\}} \rho_{shgr} \leq U_{shg} \overline{P_g} \tag{8}$$

(repeated in Eq. A.8), where ρ_{shgr} is the reserves of type r from technology g and U_{shg} is an integer variable representing the number of units committed. In addition, a range of system constraints (e.g. load balance and reserve requirements) and generator constraints (including minimum stable generation, minimum up/down times and ramp rates) are

included, with the full set of constraints presented in Appendix A.

A full year is modelled, with each day simulated individually, mimicking the day-ahead market/commitment process of many power systems. An hourly time resolution is used and a 24-hour look-ahead period into the next day is also included, to avoid any early end-effects.

The model is stochastic in that commitment decisions for nuclear, coal and CCGT must be identical across different possible scenarios of demand, wind and solar forecasts, the error of which grows in time. Forecasts are updated at the start of each day and are produced with an Auto-Regressive Moving Average (ARMA) model.

Upon completion of the UC run, an economic dispatch (ED) sub-model is used with the commitment variables fixed to the values from the UC run, to determine energy and reserve prices. These are obtained from the shadow prices of the constraints on the power balance and on the reserve requirements respectively. Other than treating the commitment variable as a fixed parameter, this model includes the same constraints as the UC sub-model.

2.3.2. ED-Only Sub-Model

To understand the importance of UC constraints on their own, another version of this sub-model is run, called the ED-Only sub-model, that does not include constraints which require an integer commitment variable.

In the ED-Only sub-model, the variable representing the number of units committed, U_{shg} is set equal to the number of units built, B_g. For example, Eq. (8) now becomes

$$p_{shg} + \sum_{r \in \{\overline{\mathrm{p}},\overline{\mathrm{s}},\overline{\mathrm{t}}\}} \rho_{shgr} \leq B_g \overline{P_g} \tag{9}$$

Constraints involving the commitment variable U_{shg} are also not included, e.g. minimum stable generation or minimum up/down time constraints. The full set of constraints is presented in Appendix A.

This model is then an operational analogue to the GE model described in Section 2.2, in that it includes the same types of constraints, except that investment decisions are fixed. It should be noted that as UC constraints are not included in the ED-Only sub-model, C^{St}_{sg} will be zero in its optimal solution.

2.3.3. Inertia and Rate of Change of Frequency

This paper investigates the impact of a RoCoF constraint on generator dispatch and financial performance. Maximum RoCoF occurs immediately following a disturbance, and is equal to [42]

$$\mathrm{RoCoF}^{\max} = \frac{P^{\mathrm{dist}} f_0}{2H^{\mathrm{sys}}}, \tag{10}$$

in which P^{dist} is the size of the disturbance, f_0 is the reference frequency, and H^{sys} is the amount of inertia in the system. The UC+ED sub-model therefore requires sufficient inertia to be available to limit RoCoF through the following constraint:

$$2\mathrm{RoCoF}^{\max}(H^{\mathrm{on}}_{sh} - H^{\max}_{sh}) \geq P^{\max}_{sh} f_0. \tag{11}$$

Here, H^{on}_{sh} is the total inertia prior to the contingency event, for scenario s, period h. $P^{\max}_{sh}$ and $H^{\max}_{sh}$ are the largest credible contingency and largest single online source of inertia respectively, with both being determined dynamically within the optimisation. Note that the former is set to be at least as large as the capacity of the largest online unit, but with a static lower bound (to represent a transmission/load-driven event). The formulation of these constraints is defined in Eqs. (A.27 - A.31) in Appendix A.

Three levels of this RoCoF constraint are examined, defined as follows:

i) **1 Hz/s**: A maximum RoCoF constraint of 1 Hz/s which is the current rate for which generators in the NEM must be capable of continuous operation [43].
ii) **0.5 Hz/s**: A RoCoF constraint of 0.5 Hz/s as was used in the Irish system [44].
iii) **Unconstrained**: No constraint on RoCoF is applied.

The credible contingency size has a lower bound of 200 MW, but if a unit with a capacity larger than this is committed (e.g. a nuclear unit), then that capacity becomes the credible contingency. The 1 Hz/s constraint and the 200 MW contingency size are used in all simulations unless otherwise specified.

2.4. Technical Input Data

Data for operational constraints such as minimum stable generation, minimum on times, ramp rates, reserve capability, and start-up fuel-use is from Meibom et al. [17]. All thermal technologies are assumed to have an inertial constant of 6s,

as used in Ahmadyar et al. [11]. Battery storage has four hours of storage capacity, a round-trip efficiency of 85% [38], and reserve capability equal to its capacity [4]. Batteries and VRG are modelled as not providing inertia. Input data for each technology is shown in the tables within Appendix B.

2.5. Implementation

The GE and UC optimization sub-models were written in the General Algebraic Modeling System (GAMS) [45] language, and solved using CPLEX 12.1. The UC+ED sub-model was the most computationally demanding sub-model, with a run-time of one to four days on a standard desktop computer for a year-long simulation. An optimality tolerance of 0.5% was used in the mixed-integer simulations.

3. Results

We first compare performance of the five fleets in the UC+ED and ED-Only sub-models in Section 3.1, and then turn to the impact of the three levels of the RoCoF constraint in Section 3.2.

3.1. Importance of UC Constraints

3.1.1. Capacity and Energy Decisions

Before comparing the sub-models, we present the capacity and annual energy across fleets in Figure 2. In the wind fleet a REC price of $80/MWh is required for any wind capacity, and there is no solar capacity. This is due to the high capital cost of renewables in the 2012 dataset. Nonetheless, at a $100/MWh REC price, wind supplies 40% of annual energy.

In contrast, solar is present even with no environmental policy in those fleets which use the 2050 dataset (the two solar fleets and the storage fleet). Solar capacity then grows with increasing carbon or REC price. In the solar fleet [RPS], once the annual solar energy contribution exceeds 20%, significant curtailment means wind is then built, with similar behaviour in the storage fleet.

A carbon price of $40/t replaces all coal capacity with CCGT in the solar fleet [CP] and the nuclear fleet. In the latter, nuclear provides approximately 75% of energy once the carbon price reaches $80/t. Coal generation is removed in the fleets with a RPS, not because that policy directly affects coal, but because the introduction of wind and solar make the net-load duration curve more peaky, such that less baseload capacity is required.

Finally, storage is never optimal at a $500/kWh-capital cost, but at $250/kWh (storage fleet), a small amount is built even without environmental policy. This then allows more solar capacity compared with the two solar fleets. As the REC price increases and VRG grows, storage becomes increasingly valuable as it reduces VRG curtailment. This fleet then has more renewable capacity and less thermal capacity than any other.

3.1.2. Sample Dispatch

Figure 3 shows examples of a four-day dispatch schedule for each fleet, at an $80/MWh REC price or an $80/t carbon price. The same four days from the UC+ED (left) and ED-Only (right) sub-models are shown. In the wind fleet and nuclear fleet there are only minor differences when UC constraints are included; namely that coal or nuclear generation is reduced to allow CCGT units to run at their minimum generation at times of low demand/high renewable production.

But differences are more pronounced in the other fleets, each of which is characterised by substantial solar capacity. As the typical daily solar profile is more concentrated than the typical wind profile, the former has a more severe impact on UC constraints and substantial VRG curtailment occurs. Wind generation is curtailed before solar as it has higher variable costs (see Table B.4).

Finally, there are differences in the dispatch of storage units in the storage fleet, e.g. between hours 40-50. As storage cannot continuously generate at full capacity, CCGT units are also dispatched. First, consider the ED-Only schedule. Without UC constraints, start-up costs are zero and the objective function is only influenced by the fuel costs, VOM costs, and the REC price (assuming no unserved energy/reserve). Therefore, any solution that utilises all of the stored energy, and serves the remaining demand with energy from CCGT results in the same total cost. The solution that is produced in the ED-Only sub-model is infeasible and/or expensive when UC constraints and start-up costs are introduced. In UC+ED sub-model, dispatch of the CCGT and storage units is therefore less volatile.

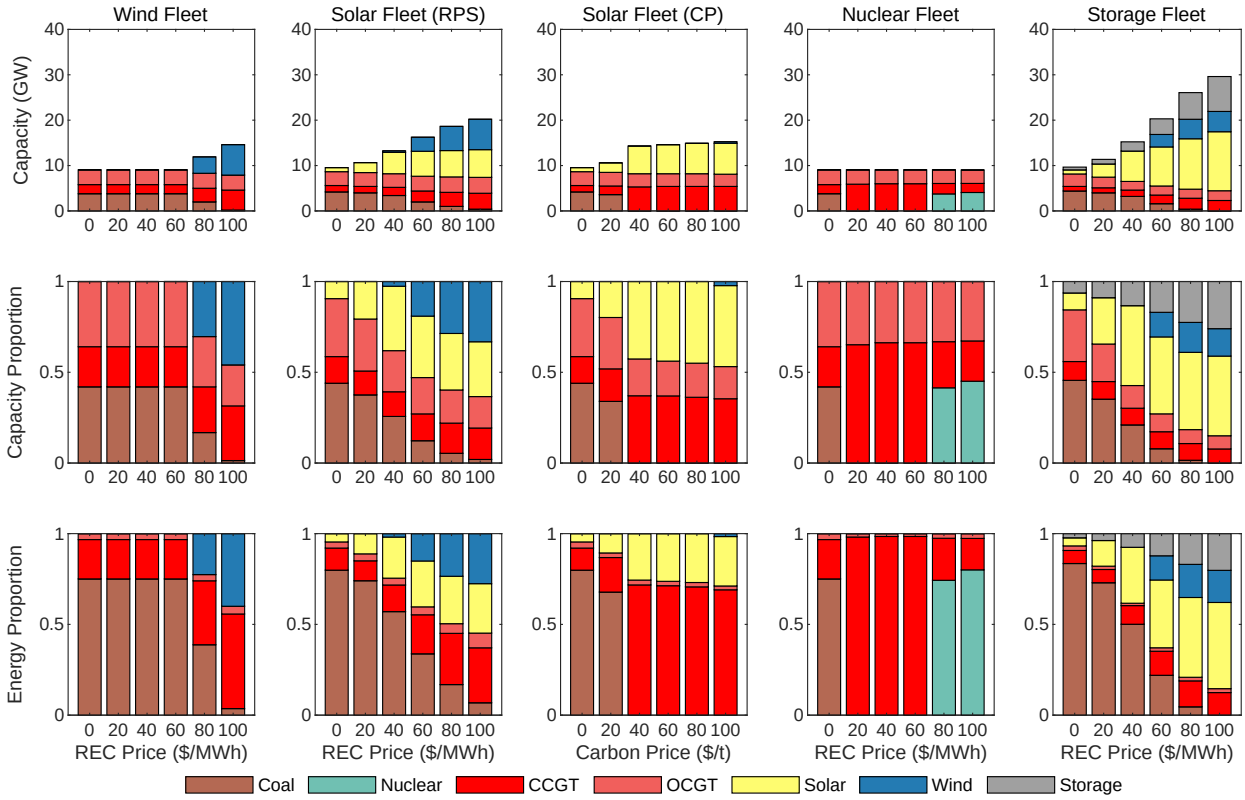

Figure 2: Capacity, capacity proportion, and energy proportion for each fleet and environmental policy price from the GE sub-model.

3.1.3. Average System Cost

We now examine the system average cost (SAC) of each fleet,

$$\hat{C}^{\mathrm{Av}} = \frac{\sum_{g} \left(\hat{C}_g^{\mathrm{Fi}} + \hat{C}_g^{\mathrm{Va}} + \hat{C}_g^{\mathrm{St}} \right) + \hat{C}^{\mathrm{Un}}}{\hat{D}}. \qquad (12)$$

Here, the first bracketed term represents total annual fixed costs (i.e. the annualised capital cost and FOM cost) for technology g, and remaining terms have the same meaning as for Eq. 1, except that the hat indicates that the quantities have been summed over all 365 simulated days, and averaged over all scenarios. Figure 4 shows the SAC for both the ED-Only and UC+ED sub-models and Figure 5a shows the difference in this cost between the two sub-models.

The wind fleet and nuclear fleet have the smallest difference between the SAC produced by the two sub-models. These fleets have differences of at most \$1.23/MWh (P^{Re}=\$100/MWh) and \$0.90/MWh (P^{Ca}=\$100/t) respectively. As the nuclear fleet is entirely dispatchable, this similarity is expected. However, the difference in the wind fleet is also small, even with wind energy exceeding 40% of annual demand. This suggests that there is little value in including UC for planning decisions in such fleets. As a comparison, Palmintier & Webster [19] found that UC constraints had more impact for fleets with wind capacity, but other units in their fleets had less flexible UC parameters than those used here.

The two solar fleets and the storage fleet exhibit greater differences between the SAC of the two sub-models. As expected, the most extreme difference occurs at the highest level of policy (P^{Re} = \$100/MWh or P^{Ca} = \$100/t). These differences are \$6.23/MWh (solar fleet [RPS]), \$4.40/MWh (solar fleet [CP]) and \$4.83/MWh (storage fleet), substantially larger than the wind fleet or nuclear fleet. This suggests that including UC constraints in the planning problem is more important for fleets with significant solar generation, e.g. for fleets with more

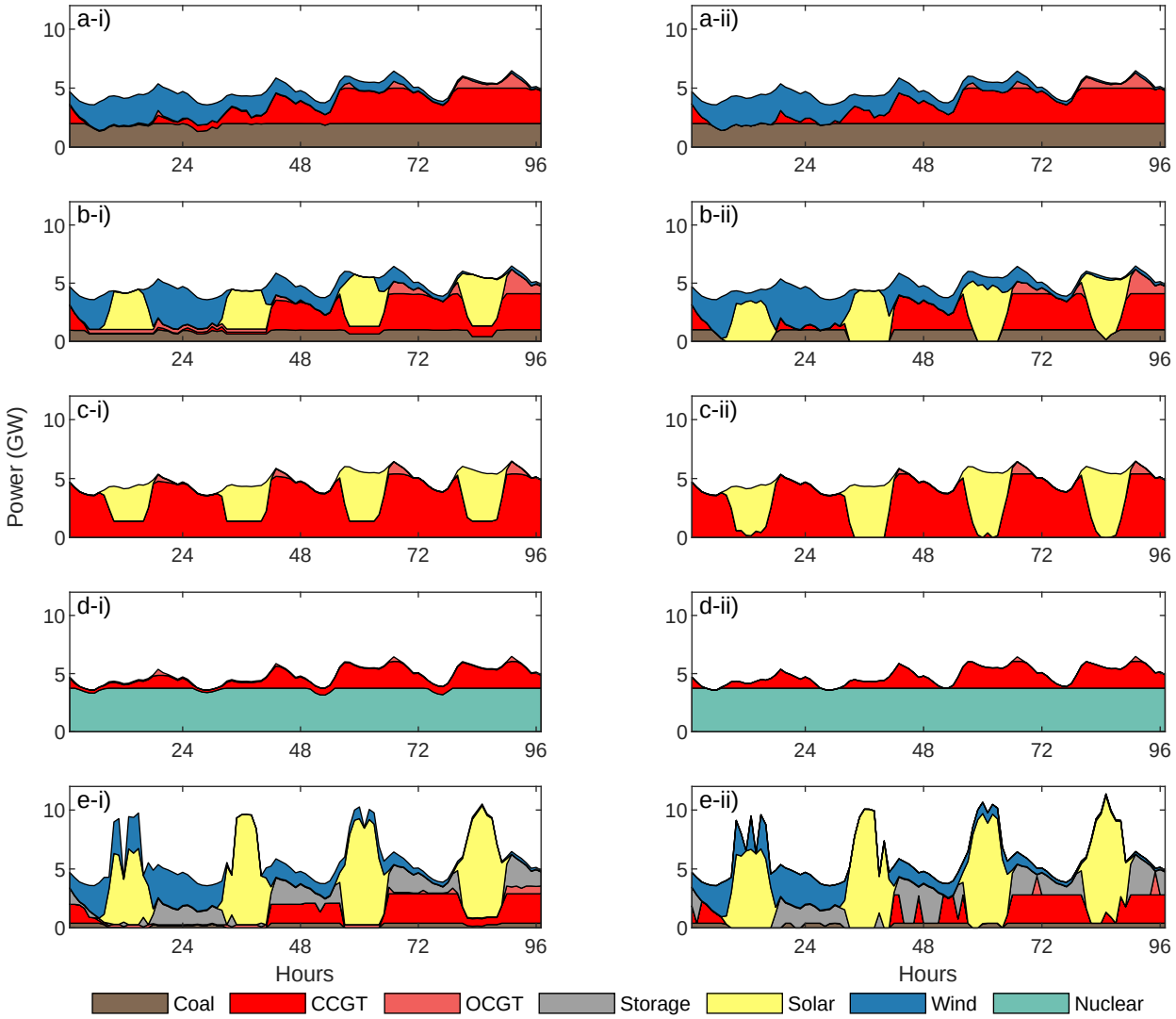

Figure 3: Dispatch over four days for a) the wind fleet b) the solar fleet [RPS] c) the solar fleet [CP] d) the nuclear fleet and e) the storage fleet, from i) the UC+ED sub-model and ii) the ED-Only sub-model, with an $80/MWh REC price (a, b, e), or a $80/t carbon price (c, d).

than 20% solar by annual energy (see Figure 2). A larger difference in system average cost occurs in the solar fleet [RPS] than in the solar fleet [CP]. The former has both significant wind capacity and (relatively inflexible) coal capacity, which the latter does not. Finally, the storage fleet has significantly more VRG generation than any other fleet, but does not produce higher cost differences between the two sub-models, indicating that energy storage can reduce the impacts of UC constraints.

3.1.4. Carbon Intensity & Renewable Energy

Figure 6 shows the carbon intensity and renewable energy from each fleet in the two sub-models. Figures 5b & 5c also highlight the difference across the sub-models of these quantities. Because the wind fleet and nuclear fleet use the 2012 dataset (Table 1), they have higher carbon intensity than other fleets without a RPS/carbon price. Again, differences between the sub-models is most significant for the three fleets with significant solar capacity, showing a decrease in the energy contribution

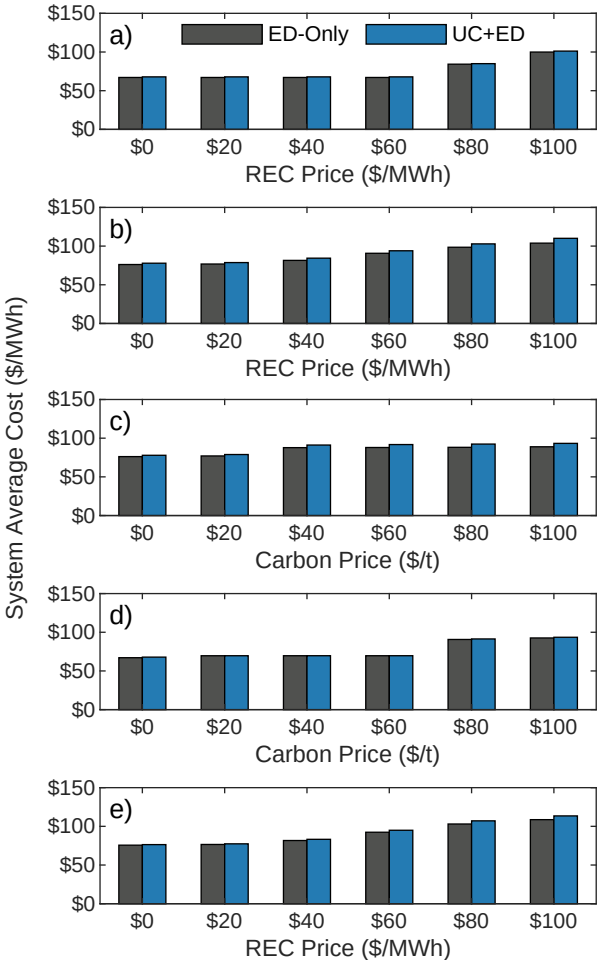

Figure 4: System average cost for a) the wind fleet b) the solar fleet [RPS] c) the solar fleet [CP] d) the nuclear fleet and e) the storage fleet.

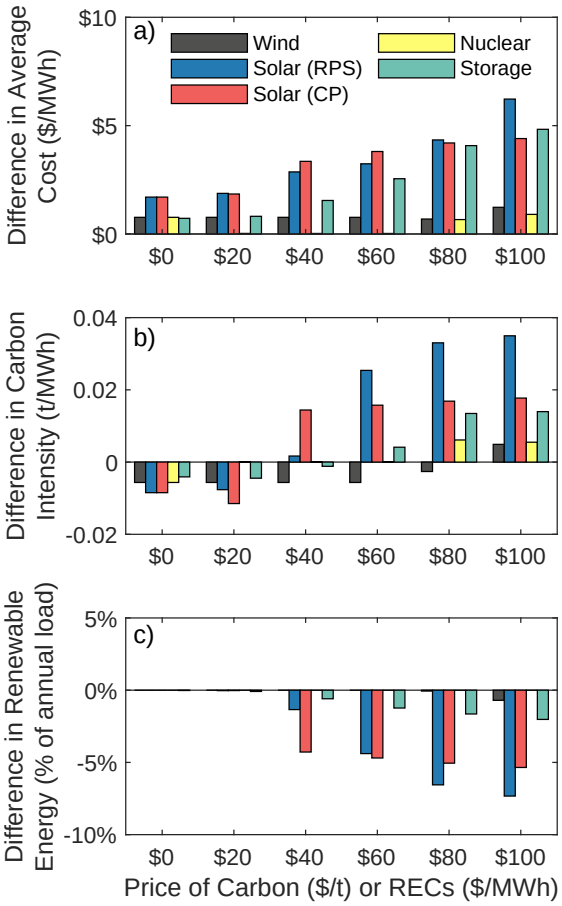

Figure 5: Difference in the UC+ED and ED-Only sub-model predictions of a) system average cost b) carbon intensity and c) renewable energy, for each fleet. Positive values indicate the UC+ED sub-model's value is greater.

from VRG by over 5% of annual demand.

Earlier, it was mentioned that the higher variable costs of wind means it is curtailed before solar. Interestingly, in the solar fleet [CP] with an \$80/MWh REC price, the capacity factor of wind decreases by 3.7% points when UC constraints are applied compared with a decrease of 2.2% points for solar. This indicates that curtailment usually takes place during the daylight hours, with wind being curtailed down to zero output, and then some solar also needing to be curtailed.

3.1.5. Financial Performance

We now turn to the financial performance of generating technologies. The profit of a technology over a day is calculated as

$$\begin{aligned}\Pi_g = &\sum_{sh} \pi_s p_{shg} \left(\mu^{\mathrm{e}}_{sh} - 3.6 c^{\mathrm{FC}}_g/\eta^{\mathrm{th}}_g - c^{\mathrm{VOM}}_g\right) \\ &+ \sum_{r} \pi_s \rho_{shgr} \mu^{\mathrm{r}}_{shr} \\ &+ \sum_{sh} \pi_s p_{shg} \left(\Omega^{Re}_g P^{\mathrm{Re}} - \mathrm{E}_g P^{\mathrm{Ca}}\right) \\ &- \sum_{sh} \pi_s \Omega^{St}_g \frac{1-\eta^{\mathrm{rt}}_g}{\eta^{\mathrm{rt}}_g} e_{shg} \hat{F}^{\mathrm{Re}} P^{\mathrm{Re}}.\end{aligned} \tag{13}$$

In this equation, the first line is the total wholesale energy payment (at the energy price, μ^{e}_{sh}) less the fuel and VOM costs of producing that energy. The second line is the wholesale payment for being enabled for reserves, at the reserve price μ^{r}_{shr}. The

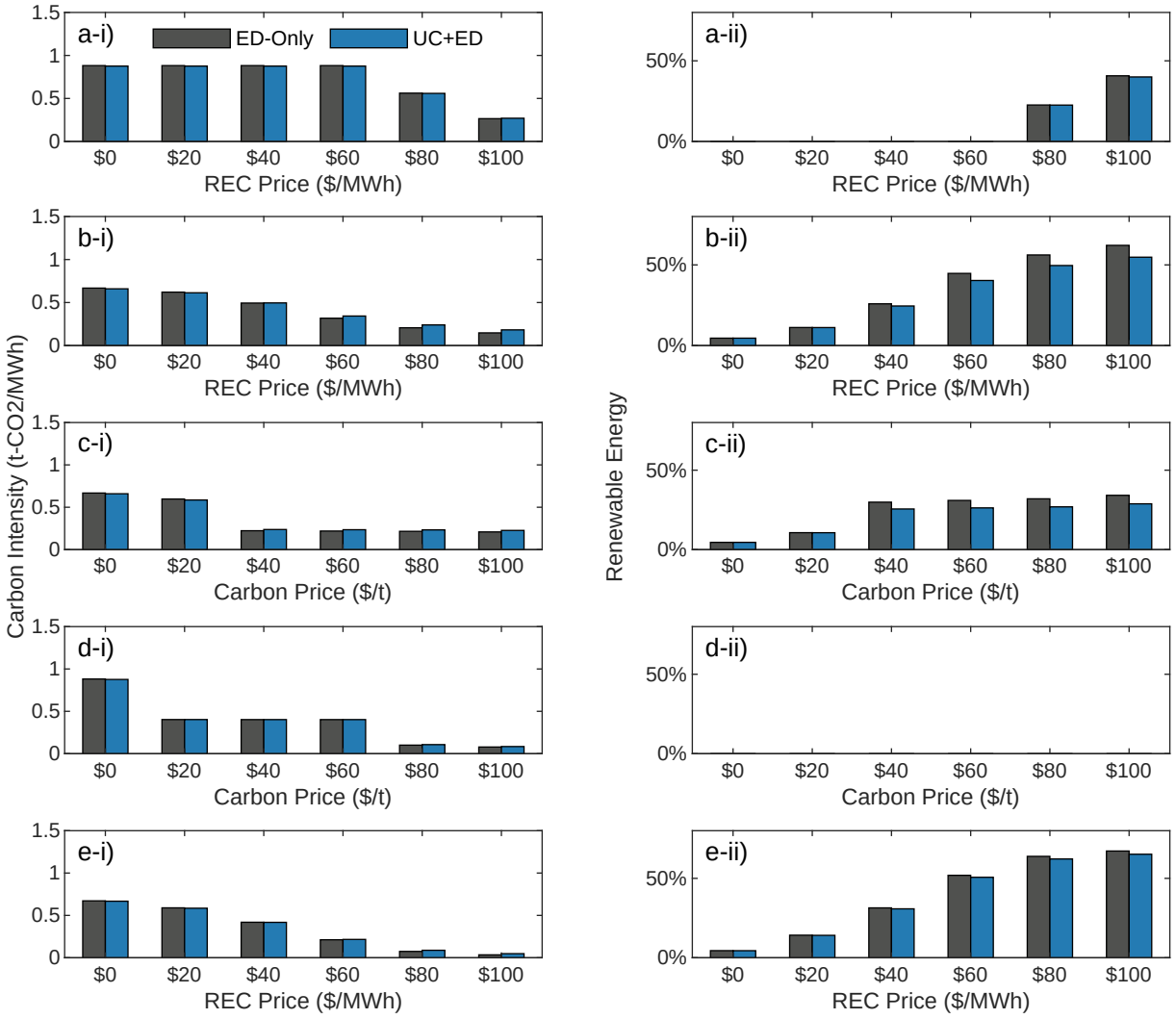

Figure 6: i) Carbon intensity and ii) renewable energy (as a percentage of annual demand) for a) the wind fleet b) the solar fleet [RPS] c) the solar fleet [CP] d) the nuclear fleet and e) the storage fleet.

third line represents REC payments to renewable technologies (Ω_g^{Re} is a parameter which is unity for renewable technologies, and zero otherwise), and charges to generators for their emissions (E_g is the emissions intensity of technology g). The final line is a charge to storage units (Ω_g^{St} is unity for storage only, zero otherwise), requiring the purchase of REC certificates for their round-trip losses over the annual proportion of renewable energy, $\hat{F}^{\mathrm{Re}}$.

This daily profit is then summed over all simulated days to determine the annual profit $\hat{\Pi}_g$. Next, the IRR is calculated as the value of the discount rate, d, which sets the sum of discounted cashflows (i.e. annual profit) over the technology's life (L_g) equal to its capital cost, i.e.

$$\sum_{y}^{\mathrm{L}_g} \frac{\hat{\Pi}_g - \hat{c}_g^{\mathrm{FOM}}\overline{P_g}}{(1+d)^y} = \hat{c}_g^{\mathrm{Cap}}\overline{P_g}. \tag{14}$$

In this equation, $\hat{c}_g^{\mathrm{FOM}}$ and $\hat{c}_g^{\mathrm{Cap}}$ are the annual FOM cost and capital cost per unit of capacity, respectively. Note that we do not include the impacts of taxation. As a 10% discount rate was used to annualise technology capital costs, this is designated the hurdle rate at which point investors recover investment costs.

Figure 7 shows the IRR for each technology and fleet as calculated in the ED-Only and UC+ED sub-

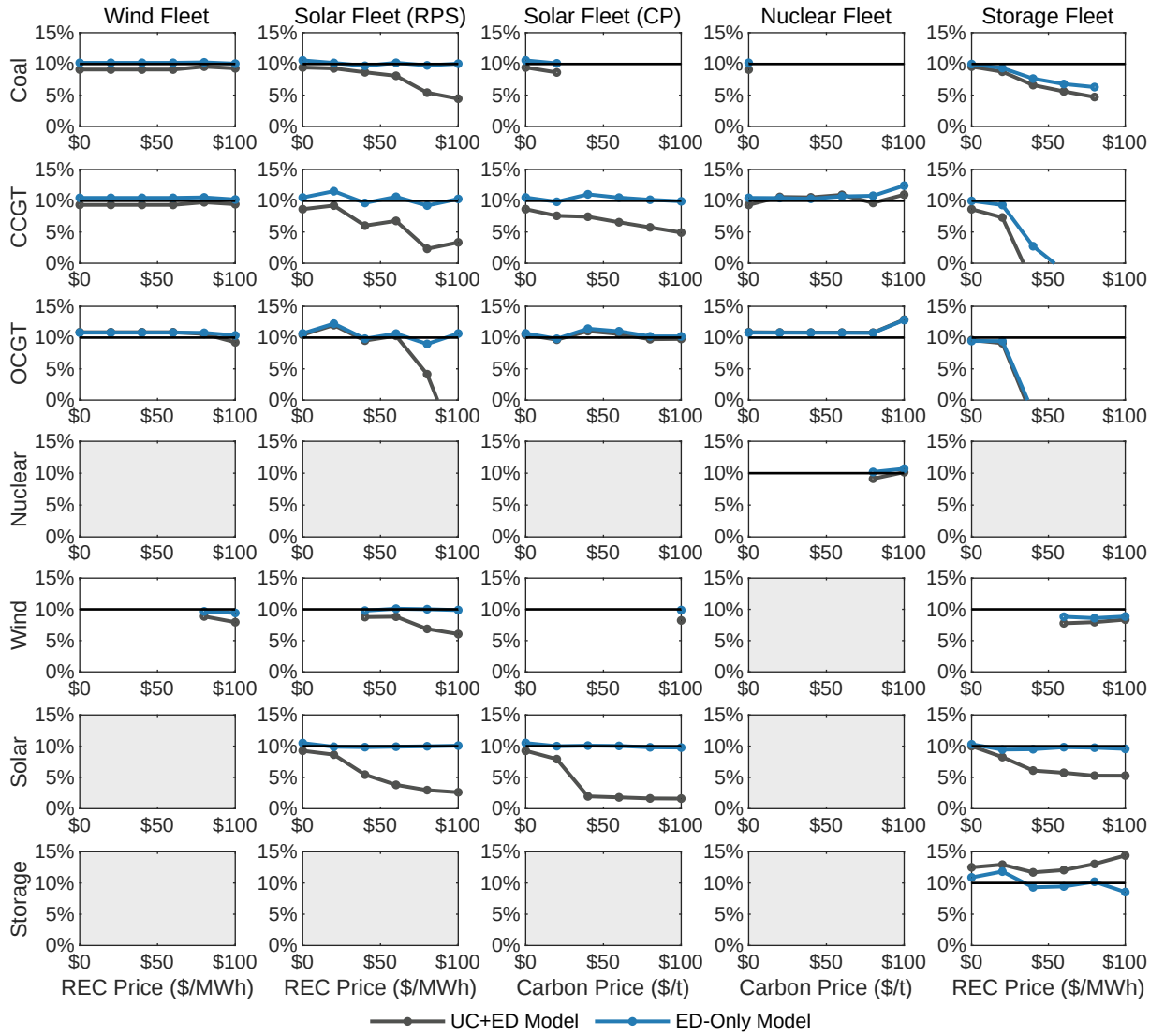

Figure 7: IRRs for each technology, fleet and sub-model. Greyed out charts indicate that the technology is never present in that fleet. The black horizontal line is the hurdle rate (10%).

models, as well as this hurdle rate (dotted line). Except in the storage fleet, the ED-Only sub-model produces returns which are approximately commensurate with the hurdle rate, whereas this is not always the case with the UC+ED sub-model.

Indeed, both the wind fleet and nuclear fleet exhibit close agreement between the two sub-models for all technologies and levels of environmental policy. This suggests these fleets are investable regardless of the environmental policy.

It is worth noting that the OCGT units have IRRs that are frequently very similar in both the ED-Only and UC+ED sub-models. This is because OCGT units have small start-up costs, and are infrequently affected by non-convex constraints as they run for only a small number of hours per year, i.e. UC constraints are less important since most/all OCGTs run at capacity when demand is high. As the most expensive form of thermal generation, revenue to cover their fixed costs comes entirely from intervals in which capacity is insufficient to supply demand and reserves, and the price is set at the MPC. This often occurs for the same number of hours in both sub-models, which is why

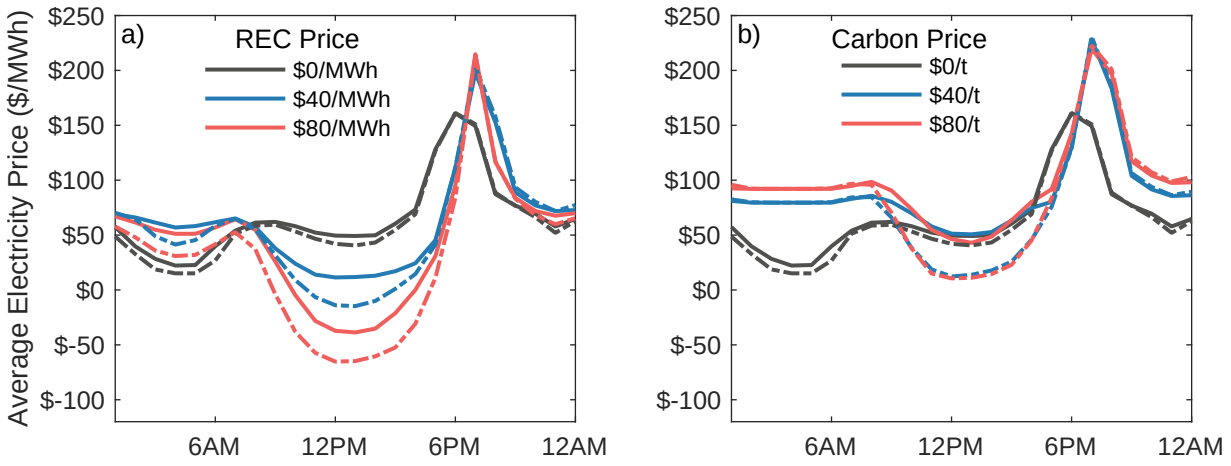

Figure 8: Average energy price by time of day in the ED-Only sub-model (solid lines) and the UC+ED sub-model (dashed-dot lines) for a) the solar fleet [RPS] and b) the solar fleet [CP].

these units have the same IRRs in both sub-models. There is also some variation in the number of intervals for which the energy price reaches the MPC. This is due to the lumpiness in unit capacity which causes variability in the IRRs of technologies, particularly those which earn the majority of their revenue in such intervals, and is another example of a non-convex constraint.

The three fleets with significant solar capacity do not produce IRRs that satisfy the 10% hurdle rate in the UC+ED sub-model, which we now examine. Figure 8 shows the average energy price by time of day for three levels of carbon/REC price in the solar fleet [RPS] and solar fleet [CP], for both sub-models. Figure 9 similarly shows the average dispatch of each technology over the day for these fleets at a \$80/MWh REC price or \$80/t carbon price respectively. As both the policy price and the solar capacity increase, two trends develop. First, the well-known duck curve [22] develops, in which the daytime net-demand and energy price are severely diminished, and daily peak demand shifts to later in the day. Importantly, this 'duck' is not solely an artefact of UC since the ED-Only results in Figures 8 and 9 feature a less extreme form of it too.

Second, the daytime energy prices produced by the sub-models diverges, with the UC+ED prices being lower as it must curtail solar energy in order to keep thermal units online above their minimum generation. Solar units are then marginal for energy, *and their SRMC sets the energy price* (with the value of RECs subtracted in their SRMC). All units generating at such times receive a lower energy price compared to the ED-Only sub-model. The impact on solar units is magnified as they also sell less energy overall due to this curtailment.

In such cases, however, it is not only solar that is impacted. Coal and CCGT receive lower revenue as they tend to be generating electricity at times when solar is curtailed, and OCGT units are required to run at minimum stable generation to provide reserves when there would otherwise be insufficient dispatchable plant online. OCGT units are chosen as they are the most flexible and have the smallest start-up costs.

We finally consider the IRRs in the storage fleet. This fleet also has significant solar capacity and the stronger duck curve with UC again provokes a difference in IRRs between the two sub-models. This benefits storage units because when the UC constraints bind, the lower daytime prices allow storage to charge at a lower energy price; they are even being paid to charge when the price is negative. Note that the CCGT and OCGT technologies perform badly in both sub-models because the storage capacity is such that the system becomes energy-limited, rather than capacity-limited, meaning there is no unserved energy, and prices never reach the MPC, unlike other fleets.

Thus, the appearance of affordable storage does not appear to solve the revenue sufficiency problem of the entire fleet. Rather, it is the introduction of the non-convex UC constraint that causes these revenue sufficiency issues. Figures 2, 7, 8 and 9 show that the 'duck curve' appears in cases with-

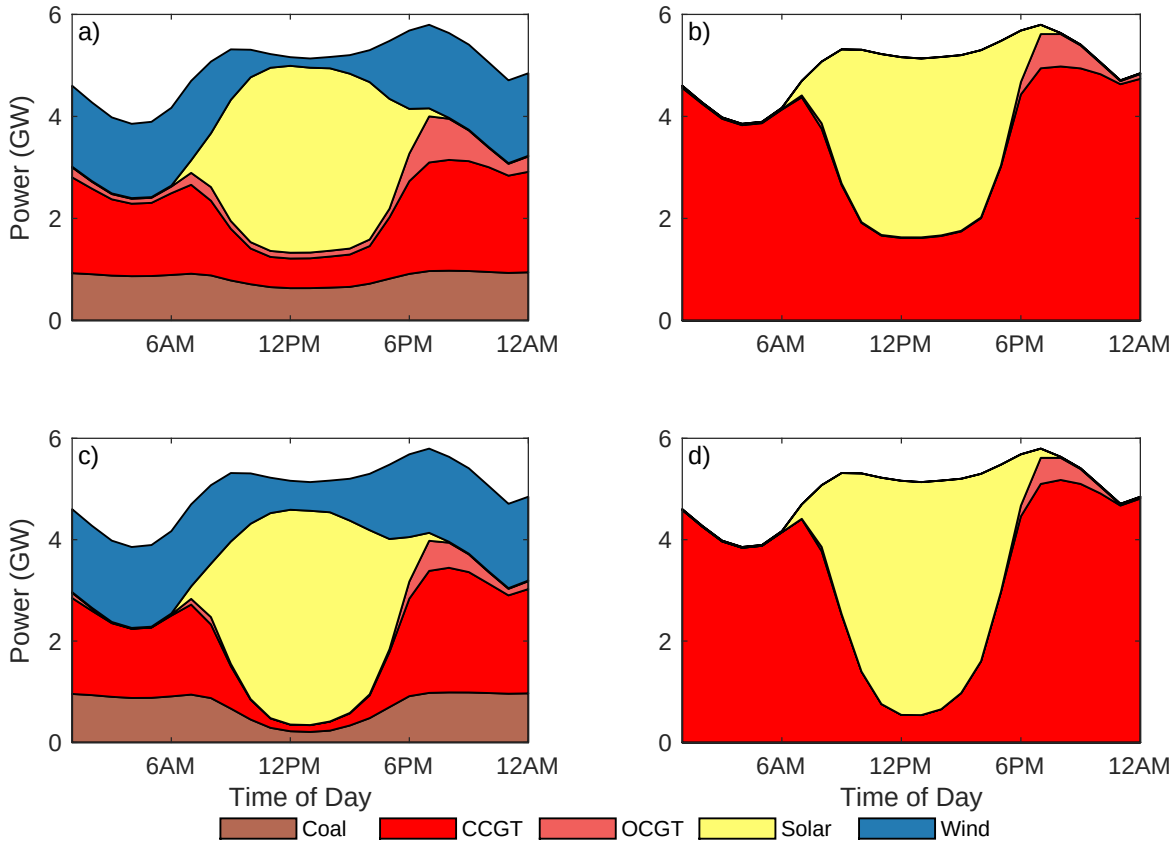

Figure 9: Average dispatch by time of day for a) solar fleet [RPS] with the UC+ED sub-model, b) solar fleet [CP] with the UC+ED sub-model, c) solar fleet [RPS] with the ED-Only sub-model and d) solar fleet [CP] with the ED-Only sub-model. In each case, the REC price or carbon price is \$80/MWh (a, c) or \$80/t (b, d) respectively.

out UC. These cases can all earn investible IRRs without UC, with solar PV uptake saturating once established because it cannibalises its own revenues during the day, as others have shown [46].

3.2. Varying the RoCoF Constraint

We now examine the impact of a RoCoF constraint on each fleet. Only the UC+ED results are considered, as inertia is dependent on the commitment of synchronous units.

3.2.1. Inertia Duration Curves

Figure 10 shows the inertia duration curves for the three constraints defined in Section 2.3.3, at policy prices of P^{Re} = \$80/MWh and P^{Re} = \$100/MWh (RPS fleets) or P^{Ca} = \$80/t and P^{Ca} = \$100/t (carbon price fleets). For all but the storage fleet, the application of the 1 Hz/s constraint does not materially impact the inertia duration curves compared with the unconstrained case. This is because fulfilling the reserves requirement simultaneously fulfils the RoCoF constraint. Reserves can only be provided by committed synchronous units (and storage), which results in a certain amount of inertia also being provided at all times. If the provision of reserves by VRG units were to become common, this wouldn't be the case.

In the storage fleet, the 1 Hz/s constraint binds for substantial periods at some of the higher REC prices shown. This is because battery storage does not provide inertia, and thus when the 1 Hz/s constraint is applied, additional thermal units need to be committed to satisfy it.

However, when the 0.5 Hz/s constraint is applied, it binds in the solar fleet [RPS], wind fleet, and the storage fleet. Interestingly, in the solar fleet [CP]

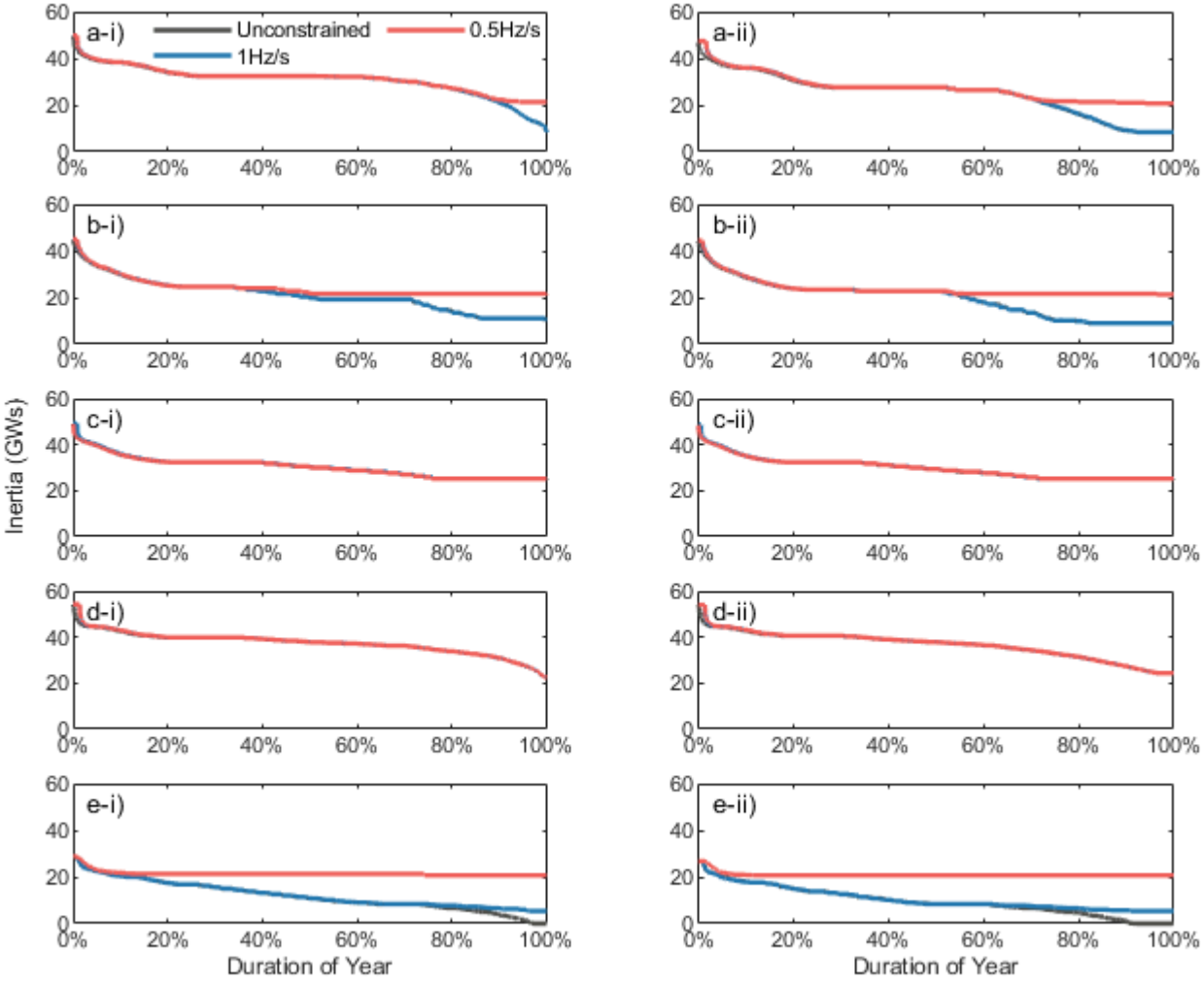

Figure 10: Inertia duration curves for a) the wind fleet b) the solar fleet [RPS] c) the solar fleet [CP] d) the nuclear fleet and e) the storage fleet, at policy levels of i) \$80/MWh (a,b,e) and \$80/t (c,d) or ii) \$100/MWh (a,b,e) and \$100/t (c,d) for the three different RoCoF constraints.

fleet, it is never binding, despite that fleet having up to approximately 40% energy from solar. This is because the carbon price replaces coal with CCGT which have a less restrictive minimum generation constraint. More of these units can be committed without incurring higher dispatch costs from curtailing VRG.

Generally, the 0.5 Hz/s constraint imposes only slightly higher costs on the system. Cost increases are largest in the storage fleet with $P^{\mathrm{Re}} =$ \$100/MWh, where the average cost increases by \$3/MWh relative to the 1 Hz/s constraint case, or \$7/MWh if including policy costs - i.e. the value of renewable energy from the REC payments.

To demonstrate how the commitment and dispatch schedules are impacted by the RoCoF constraint, Figure 11 shows the available inertia and dispatch of technologies over a four-day period with the unconstrained and 0.5 Hz/s cases for the solar fleet [RPS] with $P^{\mathrm{Re}} =$ \$80/MWh. Under the 0.5 Hz/s constraint, additional CCGT units are committed to increase available inertia. Coal, wind and solar units are all dispatched downwards to allow CCGT units to be committed at their minimum stable generation.

3.2.2. RoCoF and Financial Performance

Figure 12 shows the IRR of technologies in the wind fleet and the solar fleet [RPS], under the three RoCoF constraints. In the wind fleet, there is little

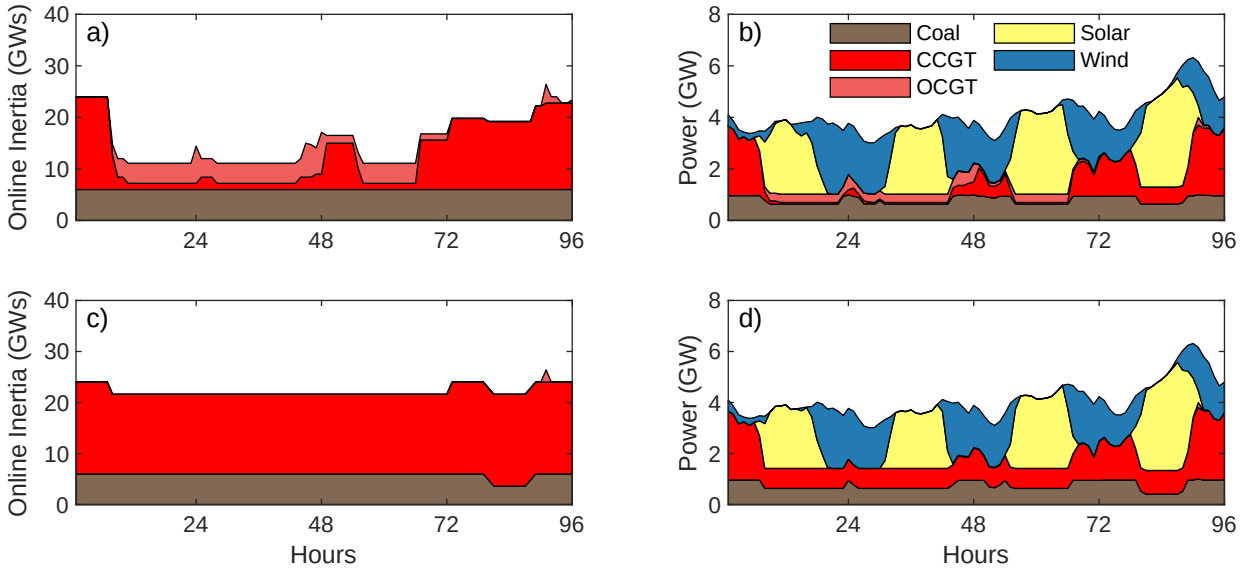

Figure 11: Online inertia and power generation from each technology for a four day period for the \$80/MWh REC price in the solar fleet [RPS]. Charts a) and b) show the inertia and power output respectively, without the RoCoF constraint, while charts c) and d) show the same quantities with the 0.5 Hz/s constraint.

variation between the three levels of constraint. In the solar fleet [RPS], we observe the same trend as in Figure 7, that is decreasing IRRs with growing VRG, with this being more or less severe with the 0.5 Hz/s or unconstrained cases respectively. However, these differences do not affect whether technologies do or do not meet their hurdle rate. Whilst the 0.5 Hz/s constraint does tend to reduce the IRR of technologies when the REC price is \$40/MWh or greater, these technologies are already uninvestable.

That said, the 0.5 Hz/s constraint can improve the IRR of OCGTs such that they almost reach their hurdle rate. This counter-intuitive result occurs because additional CCGT units are committed for inertia. As these units also provide reserves, the number of periods where OCGT units must be committed for reserves but not energy - in which they lose revenue - decreases, hence improving the OCGT IRR. For example, in this fleet with $P^{\mathrm{Re}} =$ \$80/MWh, each OCGT unit is committed for an average of 13.0% and 6.9% of intervals under the 1 Hz/s and 0.5 Hz/s constraints respectively. This result is of course not expected to be general, and should be dependent upon several parameters, including each technology's inertial constant, minimum stable generation and reserve capability, as well as system reserve and inertia requirements.

4. Conclusion

This paper examined the impact of unit commitment (UC) and rate of change of frequency (RoCoF) constraints on the performance and revenue sufficiency of decarbonising wholesale electricity markets. In general, these constraints bind with greater frequency as the uptake of wind and solar PV generation increases, although their significance also depends upon both the type of renewable generation present and the flexibility of other technologies in the market [14, 19, 20]. Consequently, different environmental policy and cost inputs were first used to produce increasingly decarbonized fleets with large differences in the uptake of wind, solar and flexible plant by using generation expansion (GE) planning that did not feature either of these constraints. The performance of these fleets was then assessed with and without UC and RoCoF constraints in a conventional economic dispatch (ED) framework.

These assessments showed that generating fleets with less than approximately 40% wind and 20% solar PV by annual generation were not significantly impacted by the application of the UC constraints. However, market performance (with UC constraints) progressively deteriorated as solar PV uptake increased beyond this limit. This was be-

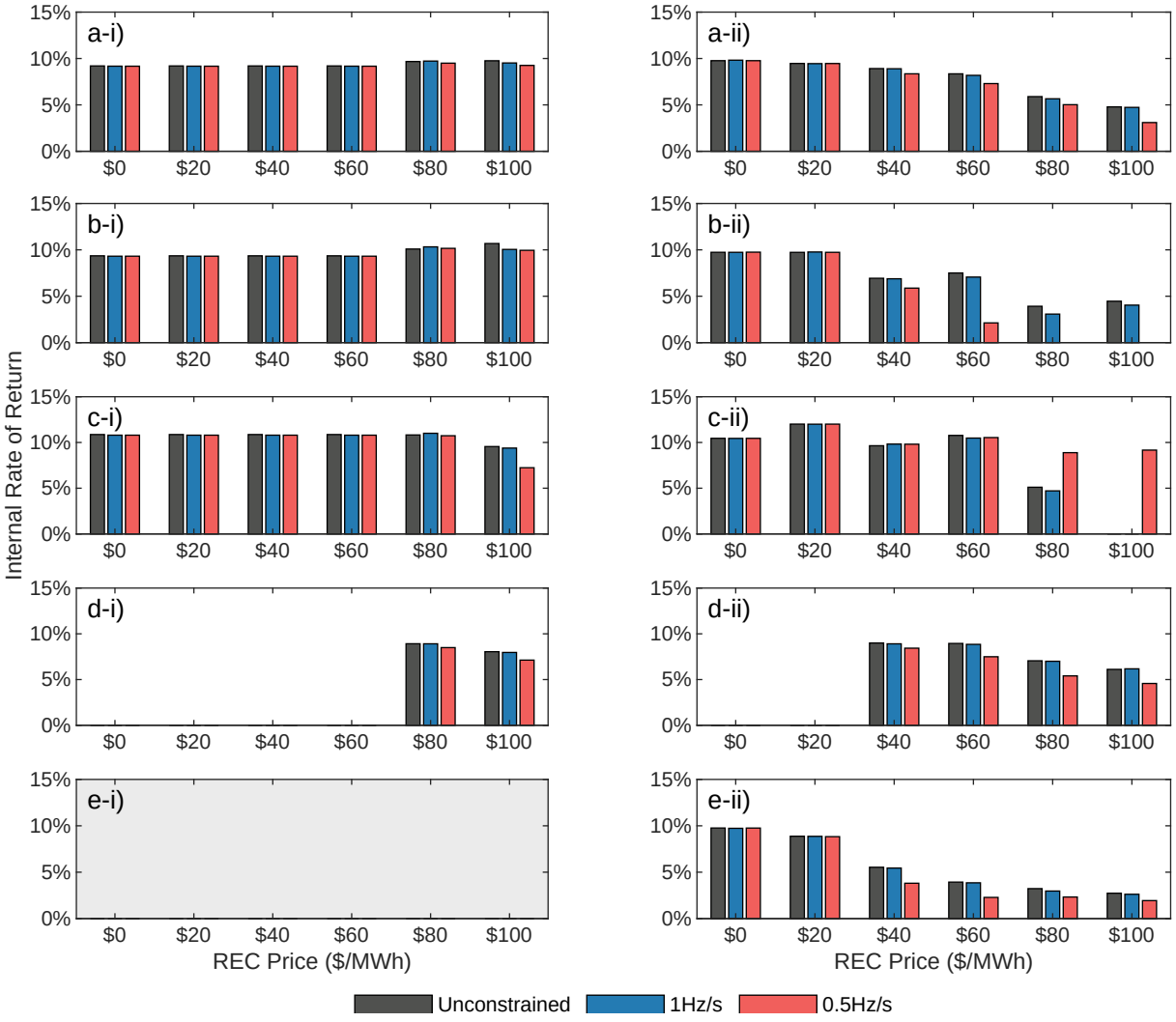

Figure 12: IRRs of a) coal, b) CCGT, c) OCGT, d) wind, and e) solar in the i) wind fleet and ii) solar fleet [RPS] fleets, with RoCoF being unconstrained or limited to 1 Hz/s or 0.5 Hz/s.

cause of the interaction between the widely discussed 'duck curve' and UC constraints, which further reduced market prices and thus returns for renewable *and* thermal generators, beyond that which would otherwise be revenue sufficient if UC constraints were not binding.

In more extreme cases, the UC constraint also required some dispatchable plant to remain online when energy prices were below their marginal costs so that they could provide various services; either inertia, reserves or ramping. Furthermore, the addition of storage did not resolve this issue because the GE model without UC over-estimated the amount of solar generation that could be scheduled. In such cases, the returns of storage plant in the ED cases with UC exceeded their cost of capital since imposition of the UC constraints meant that storage could then recharge at lower prices.

The performance of fleets under different RoCoF constraints was then examined. The 1 Hz/s constraint only affected the inertia duration curve of the fleet with a significant amount of combined solar and storage capacity. The more severe 0.5 Hz/s constraint also affected other fleets with significant wind or solar generation. However, whilst the 1 Hz/s RoCoF constraint only marginally impacted the internal rates of return (IRR) of all types of generation in all cases, the 0.5 Hz/s RoCoF con-

straint only worsened the financial performance of wind, solar, coal and CCGT when their IRRs were already adversely impacted by UC. The 0.5 Hz/s RoCoF constraint also improved the IRR of OCGT in cases with substantial solar as it was less frequently required to provide security services, with these being provided by CCGT instead.

When viewed together, these results suggest that conventional GE planning tools without UC and RoCoF constraints should produce fleets that can transact via an efficient wholesale market if there is less than approximately 40% wind and 20% solar PV by annual generation. In this case, system average costs should match average prices, all generating units' IRRs should match the cost of capital used in the GE plan and costs to consumers should be minimised. However, the inclusion of UC, RoCoF and potentially other reliability and security considerations may be required in GE planning tools beyond these approximate limits of renewable generation.

Appendix A. Model Formulation

Appendix A.1. Nomenclature

The nomenclature for the UC+ED and ED-Only sub-models is presented below.

Sets

$g \in \mathcal{G}$	Generating technologies.
$\mathcal{G}_R \subset \mathcal{G}$	Renewable technologies.
$\mathcal{G}_S \subset \mathcal{G}$	Storage technologies.
$\mathcal{G}_D \subset \mathcal{G}$	Dispatchable technologies.
$\mathcal{G}_F \subset \mathcal{G}$	Flexible technologies.
$\mathcal{G}_I \subset \mathcal{G}$	Inflexible technologies.
$r \in \mathcal{R}$	Reserves; primary raise/lower ($\bar{p}, \underline{p}$), secondary raise/lower ($\bar{s}, \underline{s}$), and tertiary raise ($\bar{t}$).
$h \in \mathcal{H}$	Time periods; 1,...,48.
$s \in \mathcal{S}$	Scenarios (of wind, solar or demand forecasts).

Parameters

D_{sh}	Electricity demand in period h, scenario s (MW).
$\overline{w}_{shg}$	Intermittent resource availability in period h for technology $g \in \mathcal{G}_R$, scenario s (fraction of capacity).
P^{Ca}	Carbon price ($/$t_{CO_2e}$).
P^{Re}	REC Price ($/MWh).
P^{MPC}	Market price cap ($/MWh).
π_s	Probability of scenario s.
R_r	Required quantity of reserve r (MW).
$\overline{P_g}$	Unit capacity of technology g (MW).
c_g^{FC}	Fuel cost of technology g ($/GJ).
c_g^{VOM}	VOM cost of technology g ($/MWh).
c_g^{U}	Cost of starting a unit of technology g ($).
c_g^{D}	Cost of shutting down a unit of technology g ($).
B_g	Number of units of technology g.
η_g^{th}	Thermal efficiency of technology g.
η_g^{rt}	Round-trip efficiency of storage technology $g \in \mathcal{G}_S$.
$\underline{P_g}$	Minimum stable generation of technology g (MW).
Q_g	Ramp rate of technology g (fraction of capacity per hour).
M_g^{up}	Minimum up time for technology g (hours).
M_g^{do}	Minimum down time for technology g (hours).
$\overline{R}_{gr}$	Reserve capability for reserve r from technology g (MW).
E_g	Emissions intensity of technology g ($t_{CO2}/MWh).
$\mathrm{RoCoF}^{\max}$	Maximum allowable RoCoF (Hz/s).
f_0	System frequency (Hz).
H_g	Inertial constant of technology g (s).
l_g^0	Initial storage level for $g \in \mathcal{G}_S$ as taken from the last period of the previous day (MWh).
T_g	Storage duration of storage technology $g \in \mathcal{G}_S$ (hours/MW).
P^{low}	Lower bound on the largest credible contingency size (MW).

Variables

C^{To}	Total cost ($).
C_{sg}^{Va}	Total variable cost of electricity, from technology g in scenario s ($).
C_{sg}^{Ca}	Total cost of carbon emissions from technology g in scenario s ($).
C_{sg}^{Re}	Total cost of purchasing RECs from technology g in scenario s ($).
C_{sg}^{St}	Total costs of start-up/shut-down events from technology g in scenario s ($).
C_s^{Un}	Total cost of unserved energy and reserves in scenario s ($).
u_{sh}^{e}	Unserved energy in period h, scenario s (MW).
u_{shr}^{r}	Unserved reserve (type r), in period h, scenario s (MW).

p_{shg} Power generated by technology g in period h scenario s (MW).

ρ_{shgr} Reserve enablement (type r) for technology g in period h in scenario s (MW).

V_{shg} Variable which is one if storage technology $g \in \mathcal{G}_S$ is charging in period h, zero otherwise (binary).

l_{shg} Energy available in storage technology $g \in \mathcal{G}_S$ in period h, scenario s (MWh).

e_{shg} Storage charging rate of storage technology $g \in \mathcal{G}_S$ in period h (MW)

H^{on}_{sh} System inertia in period h (MW.s).

$H^{\max}_{sh}$ Largest single online source of inertia in period h (MWsec).

$P^{\max}_{sh}$ Largest credible contingency in period h (MW).

U_{shg} Number of committed units of technology g in period h, scenario s (integer).

U'_{hg} Number of committed units of inflexible technology $g \in \mathcal{G}_I$ in period h (integer).

U^1_{shg} Variable which is one if any units of technology g are committed in period h, scenario s, zero otherwise (binary).

S^{U}_{shg} Number of units of technology g started up in period h, scenario s (integer).

S^{D}_{shg} Number of units of technology g shut down in period h, scenario s (integer).

μ^{e}_{sh} Price of energy in period h, scenario s (\$/MWh).

μ^{r}_{shr} Price of reserves (type r) in period h, scenario s (\$/MW).

Appendix A.2. UC+ED Model

The objective function of the UC+ED sub-model is presented in Eq. (1), and constraints defining cost terms are shown in Eqs. (2) - (7). In addition, the UC+ED sub-model also includes the following constraints:

$$\sum_g p_{shg} + u^{\text{e}}_{sh} = D_{sh} + \sum_{g \in \mathcal{G}_S} e_{shg}/\eta^{\text{rt}}_g; \quad (\mu^{\text{e}}_{sh}), \tag{A.1}$$

$$\sum_g \rho_{shgr} + u^{\text{r}}_{shr} \geq R_r; \quad (\mu^{\text{r}}_{shr}), \tag{A.2}$$

$$U_{shg} \leq B_g, \tag{A.3}$$

$$S^{\text{U}}_{shg} = U_{shg} - U_{s(h-1)g} + S^{\text{D}}_{shg}, \quad g \in \mathcal{G}_D \setminus \mathcal{G}_S, h > 1, \tag{A.4}$$

$$U_{shg} = U'_{hg}, \quad g \in \mathcal{G}_I, \tag{A.5}$$

$$U_{shg} \geq \sum_{\substack{h^{D\prime} > h - M^{\text{up}}_g \\ h^{D\prime} \leq h}} S^{\text{U}}_{sh^{D\prime}g}, \quad g \in \mathcal{G}_I, \tag{A.6}$$

$$B_g - U_{shg} \geq \sum_{\substack{h^{D\prime} > h - M^{\text{do}}_g \\ h^{D\prime} \leq h}} S^{\text{D}}_{sh^{D\prime}g}, \quad g \in \mathcal{G}_I, \tag{A.7}$$

$$p_{shg} + \sum_{r \in \{\bar{\text{p}},\bar{\text{s}},\bar{\text{t}}\}} \rho_{shgr} \leq U_{shg}\overline{P_g}, \quad g \in \mathcal{G}_I, \tag{A.8}$$

$$p_{shg} - \sum_{r \in \{\underline{\text{p}},\underline{\text{s}}\}} \rho_{shgr} \geq U_{shg}\underline{P_g}, \quad g \in \mathcal{G}_D \setminus \mathcal{G}_S, \tag{A.9}$$

$$p_{shg} + \sum_{r \in \{\bar{\text{p}},\bar{\text{s}}\}} \rho_{shgr} \leq U_{shg}\overline{P_g} \quad g \in \mathcal{G}_F, \tag{A.10}$$

$$p_{shg} + \sum_{r \in \{\bar{\text{p}},\bar{\text{s}},\bar{\text{t}}\}} \rho_{shgr} \leq B_g\overline{P_g} \quad g \in \mathcal{G}_F, \tag{A.11}$$

$$\rho_{shgr} \leq \overline{R}_{gr}U_{shg}, \quad g \notin \mathcal{G}_S, r \in \mathcal{R} \setminus \bar{t} \tag{A.12}$$

$$\rho_{shgr} \leq \overline{R}_{gr}U_{shg} \quad g \in \mathcal{G}_I, r = \bar{t}, \tag{A.13}$$

$$\rho_{shgr} \leq \overline{R}_{gr}B_g \quad g \notin \mathcal{G}_S, g \in \mathcal{G}_F, r = \bar{t}, \tag{A.14}$$

$$p_{shg} \leq p_{s(h-1)g} + Q_g\overline{P_g}(U_{s(h-1)g} - S^{\text{D}}_{shg}) + \overline{P_g}S^{\text{U}}_{shg} - \underline{P_g}S^{\text{D}}_{shg}, \quad g \in \mathcal{G}_D \setminus \mathcal{G}_S, h > 1, \tag{A.15}$$

$$p_{shg} \geq p_{s(h-1)g} - Q_g\overline{P_g}(U_{s(h-1)g} - S^{\text{D}}_{shg}) - \overline{P_g}S^{\text{D}}_{shg} + \underline{P_g}S^{\text{U}}_{shg}, \quad g \in \mathcal{G}_D \setminus \mathcal{G}_S, h > 1, \tag{A.16}$$

$$p_{shg} \leq \overline{w}_{shg}\overline{P_g}B_g, \quad g \in \mathcal{G}_R, \tag{A.17}$$

$$l_{shg} \leq \overline{P_g}T_gB_g, \quad g \in \mathcal{G}_S, \tag{A.18}$$

$$l_{shg} = l_{s(h-1)g} + e_{shg} - p_{shg}, \quad g \in \mathcal{G}_S, h > 1, \tag{A.19}$$

$$l_{shg} = l^0_g + e_{shg} - p_{shg}, \quad g \in \mathcal{G}_S, h = 1, \tag{A.20}$$

$$e_{shg} + \sum_{r \in \{\underline{\text{p}},\underline{\text{s}}\}} \rho_{shgr} \leq V_{shg}\eta^{\text{rt}}_g\overline{P_g}B_g, \quad g \in \mathcal{G}_S, \tag{A.21}$$

$$p_{shg} + \sum_{r \in \{\bar{\text{p}},\bar{\text{s}},\bar{\text{t}}\}} \rho_{shgr} \leq (1 - V_{shg})\overline{P_g}B_g, \quad g \in \mathcal{G}_S \quad , \tag{A.22}$$

$$\rho_{shgr} \leq \overline{R}_{gr} B_g, \quad g \in \mathcal{G}_S, \tag{A.23}$$

$$e_{shg} + \sum_{r \in \{\underline{p},\underline{s}\}} \rho_{shgr} \leq \eta_g^{\mathrm{rt}} \overline{P_g} B_g, \quad g \in \mathcal{G}_S, \tag{A.24}$$

$$p_{shg} + \sum_{r \in \{\bar{p},\bar{s},\bar{t}\}} \rho_{shgr} \leq \overline{P_g} B_g, \quad g \in \mathcal{G}_S, \tag{A.25}$$

$$2\mathrm{RoCoF}^{\max}(H_{sh}^{\mathrm{on}} - H_{sh}^{\max}) \geq P_{sh}^{\max} f_0, \tag{A.26}$$

$$H_{sh}^{\mathrm{on}} = \sum_{g \in \mathcal{G}_D} U_{shg} H_g \overline{P_g}, \tag{A.27}$$

$$H_{sh}^{\max} \geq U_{shg}^1 H_g \overline{P_g}, \quad g \in \mathcal{G}_D, \tag{A.28}$$

$$P_{sh}^{\max} \geq U_{shg}^1 \overline{P_g}, \tag{A.29}$$

$$P_{sh}^{\max} \geq P^{\mathrm{low}}, \tag{A.30}$$

$$U_{shg} \leq U_{shg}^1 B_g, \tag{A.31}$$

Eq. (A.1) requires total generation and any unserved load to be equal to electricity demand plus any battery charging load in each period. Eq. (A.2) ensures reserve requirements are met.

The number of committed units from a cluster is limited by the number of units built (as determined in the GE sub-model) in Eq. (A.3). Eq. (A.4) relates start-up and shut-down events to the number of committed units, and Eq. (A.5) ensures the commitment of inflexible (coal, CCGT, nuclear) units is identical across scenarios. Eq. (A.6) requires that committed unit remain online for at least their minimum up time, M_g^{up}, with Eq. (A.7) performing the same function for their minimum down time.

Eq. (A.8) ensures that generation plus raise reserve enablement is less than each inflexible technologies' committed capacity, while Eq. (A.9) ensures that generation less lower reserves enablement is greater than minimum stable generation for all dispatchable generators. Eqs. (A.10-A.11) perform a similar function to Eq. (A.8) for flexible technologies, but allow tertiary reserve to be provided while offline. Eqs. (A.12 - A.14) limit reserve enablement to the reserve capability of each technology for each reserve type. Ramp rate limits (Q_g) are respected by Eqs. (A.15) (upward direction) and (A.16) (downward direction).

For wind and solar units, generation must be less than their resource availability in Eq. (A.17).

The level of stored energy, l_{shg}, in storage units is limited to their storage capacity in Eq. (A.18). The volumne of stored energy is adjusted for charging or discharging in Eq. (A.20) (first period) and Eq. (A.19) (all subsequent periods). Eqs. (A.21) and (A.22) limit the rates of charge/discharge and include head/foot-room for raise/lower reserves respectively. The former equation includes an adjustment for the round-trip efficiency. In these two equations, a binary variable, V_{shg}, prevents simultaneous charging and discharging (which could otherwise be economically optimal if the REC price is sufficiently high). Eq. (A.23) limits reserve enablement for storage units to their reserve capability regardless of charge/discharge mode.

As discussed in Section 2.3.3, Eq. (A.26) requires online inertia, H_{sh}^{on} to be sufficient to limit RoCoF to the maximum allowable value ($\mathrm{RoCoF}^{\max}$) in the largest credible contingency, defined by $P_{sh}^{\max}$, and without the largest source of inertia, $H_{sh}^{\max}$. Eq. (A.27) defines online inertia as the sum of the product of the committed capacity and inertial constant, H_g, of all technologies, and Eq. (A.28) defines the largest source of inertia. In Eqs. (A.29) and (A.30), the largest credible contingency is identified as the greater of the largest single online unit, and a static lower bound (representing a transmission/load contingency). U_{shg}^1 is a binary variable which is one if any units from a technology grouping are online, zero otherwise (Eq. (A.31)).

Appendix A.3. ED-Only Model

The ED-Only model replaces the variable representing the number of units committed, U_{shg}, with the number of units built, B_g, so that Eqs. (A.8) is replaced by

$$p_{shg} + \sum_{r \in \{\bar{\mathrm{p}},\bar{\mathrm{s}},\bar{\mathrm{t}}\}} \rho_{shgr} \leq B_g \overline{P_g}, \quad g \in \mathcal{G}, \tag{A.32}$$

The minimum stable generation equation (Eq. A.9) is replaced by

$$p_{shg} - \sum_{r \in \{\underline{\mathrm{p}},\underline{\mathrm{s}}\}} \rho_{shgr} \geq 0, \quad g \in \mathcal{G}_D \setminus \mathcal{G}_S. \tag{A.33}$$

The constraint requiring units to be committed to provide reserves Eq. (A.12) is replaced by

$$\rho_{shgr} \leq B_g \overline{R}_{gr}, \quad g \notin \mathcal{G}_S, r \in \mathcal{R}, \tag{A.34}$$

Finally, the ramping equations - Eqs. (A.15) and (A.16) - are simplified to

$$p_{shg} \leq p_{s(h-1)g} + Q_g \overline{P_g} B_g, \quad g \in \mathcal{G}_D \setminus \mathcal{G}_S, h > 1, \tag{A.35}$$

$$p_{shg} \geq p_{s(h-1)g} - Q_g \overline{P_g} B_g, \quad g \in \mathcal{G}_D \setminus \mathcal{G}_S, h > 1. \quad \text{(A.36)}$$

As this model assumes that all units are committed in all periods, Eqs. (A.3) - (A.7) are not included in the ED-Only model, nor are the equations which limit RoCoF - i.e. Eqs. (A.26) - (A.31)

Appendix B. Input Data

Parameters for thermal generators are shown in Tables B.2 and B.3. Table B.4 shows parameters for wind and solar PV, and Table B.5 shows parameters for the battery storage technology. Monetary quantities are specified in real 2012-13 Australian dollars.

Acknowledgements

The authors would like to acknowledge the contributions of Dr Matthew Jeppesen to the development of the optimisation models used in this work. Dr Daniel Marshman is also grateful for financial support from an Australian Postgraduate Award from the Australian Federal Government.

Declarations of interest: None

References

[1] L. Hirth, "The optimal share of variable renewables: How the variability of wind and solar power affects their welfare-optimal deployment," *The Energy Journal*, vol. 36, no. 1, 2015.

[2] V. Oree, S. Z. S. Hassen, and P. J. Fleming, "Generation expansion planning optimisation with renewable energy integration: A review," *Renewable and Sustainable Energy Reviews*, vol. 69, pp. 790–803, 2017.

[3] M. Jeppesen, M. Brear, D. Chattopadhyay, C. Manzie, R. Dargaville, and T. Alpcan, "Least cost, utility scale abatement from Australia's NEM (National Electricity Market). part 1: Problem formulation and modelling," *Energy*, vol. 101, pp. 606–620, 2016.

[4] N. Miller, D. Lew, and R. Piwko, "Technology capabilities for fast frequency response," 2017. GE Consulting. Available https://aemo.com.au/-/media/files/electricity/nem/security_and_reliability/reports/2017/2017-03-10-ge-ffr-advisory-report-final---2017-3-9.pdf?la=en&hash=468D48C40DBFF572166766F2B8A180C4.

[5] F. Milano, F. Dörfler, G. Hug, D. J. Hill, and G. Verbič, "Foundations and challenges of low-inertia systems," in *2018 Power Systems Computation Conference (PSCC)*, pp. 1–25, IEEE, 2018.

[6] P. Mancarella, S. Püschel-Løvengreen, H. Wang, M. Brear, T. Jones, M. Jeppesen, R. Batterham, R. Evans, and I. Mareels, "Power system security assessment of the future National Electricity Market," 2017. Melbourne Energy Institute (MEI). Available https://www.energy.gov.au/sites/default/files/independent-review-future-nem-power-system-security-assessment.pdf.

[7] Australian Energy Market Operator, "Integrating Utility-Scale Renewables and Distributed Energy Resources in the SWIS," March 2019. Available https://aemo.com.au/en/energy-systems/electricity/wholesale-electricity-market-wem/system-operations/integrating-utility-scale-renewables-and-distributed-energy-resources-in-the-swis.

[8] Australian Energy Market Operator, "Renewable Integration Study: Stage 1 Report," April 2020. Available https://www.aemo.com.au/-/media/files/major-publications/ris/2020/renewable-integration-study-stage-1.pdf.

[9] S. Sharma, S. Huang, and N. Sarma, "System inertial frequency response estimation and impact of renewable resources in ERCOT interconnection," in *2011 IEEE Power and Energy Society General Meeting*, pp. 1–6, IEEE, 2011.

[10] B. Hartmann, I. Vokony, and I. Táczi, "Effects of decreasing synchronous inertia on power system dynamics—overview of recent experiences and marketisation of services," *International Transactions on Electrical Energy Systems*, vol. 29, no. 12, p. e12128, 2019.

[11] A. S. Ahmadyar, S. Riaz, G. Verbič, A. Chapman, and D. J. Hill, "A framework for assessing renewable integration limits with respect to frequency performance," *IEEE Transactions on Power Systems*, vol. 33, no. 4, pp. 4444–4453, 2017.

[12] S. Püschel-Løvengreen and P. Mancarella, "Frequency response constrained economic dispatch with consideration of generation contingency size," in *2018 Power Systems Computation Conference (PSCC)*, pp. 1–7, IEEE, 2018.

[13] L. V. Villamor, V. Avagyan, and H. Chalmers, "Opportunities for reducing curtailment of wind energy in the future electricity systems Insights from modelling analysis of Great Britain," *Energy*, vol. 195, p. 116777, 2020.

[14] A. Shortt, J. Kiviluoma, and M. O'Malley, "Accommodating variability in generation planning," *IEEE Transactions on Power Systems*, vol. 28, no. 1, pp. 158–169, 2012.

[15] P. Meibom, R. Barth, B. Hasche, H. Brand, C. Weber, and M. O'Malley, "Stochastic optimization model to study the operational impacts of high wind penetrations in Ireland," *IEEE Transactions on Power Systems*, vol. 26, no. 3, pp. 1367–1379, 2010.

[16] B. C. Ummels, M. Gibescu, E. Pelgrum, W. L. Kling, and A. J. Brand, "Impacts of wind power on thermal generation unit commitment and dispatch," *IEEE Transactions on energy conversion*, vol. 22, no. 1, pp. 44–51, 2007.

[17] P. Meibom, R. Barth, H. Brand, D. Swider, H. Ravn, and C. Weber, "All island renewable grid study workstream 2b - wind variability management studies," 2007. Available http://www.eirgridgroup.com/site-files/library/EirGrid/Workstream%202B.pdf.

[18] A. Flores-Quiroz, R. Palma-Behnke, G. Zakeri, and

Parameter	Units	Coal	CCGT	OCGT	Nuclear
VOM cost	$/MWh	8	4	10	14.74
FOM cost	$/kW	60.5	10	4	34.4
Unit size (capacity)	MW	200	100	50	312.5
Ramp rate	MW/hr/MW	1.2	6.6	4.7	0.5
Minimum up time	Hours	6	4	0	48
Minimum down time	Hours	4	1	0	NA
Start-up fuel consumption	GJ/MW	61.6	1.3	0.016	NA
Shut-down fuel consumption	GJ/MW	6.16	0.13	0.002	NA
Primary reserve capability	/MW	0.065	0.0325	0.1	0.065
Secondary reserve capability	/MW	0.13	0.0925	0.2	0.13
Tertiary reserve capability	/MW	0	0	0.2	0
Inertial constant	sec	6	6	6	6
Lifetime	Years	50	40	30	60

Table B.2: Operational parameters of thermal technologies.

		Coal		CCGT		OCGT		Nuclear	
Parameter	Units	2012	2050	2012	2050	2012	2050	2012	2050
Capital cost	$/kW	$3,788	$3,762	$1,062	$1,111	$723	$755	$5,268	$5,852
Fuel cost	$GJ	$0.67	$0.61	$6.30	$10.99	$6.80	$10.99	$0.75	$0.70
Thermal efficiency	%	32.3%	43.7%	49.5%	63%	35%	46%	30.4%	30.4%
Emissions intensity	t-CO2e/MWh	1,024	759	368	315	515	429	0	0

Table B.3: Capital and fuel costs, and thermal efficiencies and emissions rates for thermal technologies, from the 2012 and 2050 AETA datasets.

Parameter	Units	Wind	Solar PV
Capacity	MW	172	100
Capital cost (2012)	$/kW	2530	3380
Capital cost (2050)	$/kW	1848	1063
FOM	$/kW	40	25
VOM	$/MWh	12	0
Lifetime	Years	25	25

Table B.4: Renewable technology parameters.

Parameter	Units	Value
Capital cost	$/kWh	$500 or $250
Capacity	MW	202.5
Hours of storage	hrs/MW	4
Round-trip efficiency	%	85%
Lifetime	Years	12

Table B.5: Storage parameters.

R. Moreno, "A column generation approach for solving generation expansion planning problems with high renewable energy penetration," *Electric Power Systems Research*, vol. 136, pp. 232–241, 2016.

[19] B. S. Palmintier and M. D. Webster, "Impact of operational flexibility on electricity generation planning with renewable and carbon targets," *IEEE Transactions on Sustainable Energy*, vol. 7, no. 2, pp. 672–684, 2015.

[20] S. Jin, A. Botterud, and S. M. Ryan, "Temporal versus stochastic granularity in thermal generation capacity planning with wind power," *IEEE Transactions on Power Systems*, vol. 29, no. 5, pp. 2033–2041, 2014.

[21] X. Chen, J. Lv, M. B. McElroy, X. Han, C. P. Nielsen, and J. Wen, "Power system capacity expansion under higher penetration of renewables considering flexibility constraints and low carbon policies," *IEEE Transactions on Power Systems*, vol. 33, no. 6, pp. 6240–6253, 2018.

[22] P. Denholm, M. O'Connell, G. Brinkman, and J. Jorgenson, "Overgeneration from solar energy in California: A field guide to the duck chart," 2015. National Renewable Energy Lab (NREL). Available https://www.nrel.gov/docs/fy16osti/65023.pdf.

[23] A. Mills and R. Wiser, "Changes in the economic value of variable generation at high penetration levels: a pilot case study of California," 2012. Lawrence Berkeley National Lab (LBNL). Available https://emp.lbl.gov/

sites/all/files/lbnl-5445e.pdf.

[24] W. P. Bell, P. Wild, J. Foster, and M. Hewson, "Revitalising the wind power induced merit order effect to reduce wholesale and retail electricity prices in Australia," *Energy Economics*, vol. 67, pp. 224–241, 2017.

[25] D. McConnell, P. Hearps, D. Eales, M. Sandiford, R. Dunn, M. Wright, and L. Bateman, "Retrospective modeling of the merit-order effect on wholesale electricity prices from distributed photovoltaic generation in the Australian National Electricity Market," *Energy Policy*, vol. 58, pp. 17–27, 2013.

[26] L. Hirth, "The market value of variable renewables: The effect of solar and wind power variability on their relative price," *Energy Economics*, vol. 38, pp. 218–236, 2013.

[27] T. Nelson, P. Simshauser, and J. Nelson, "Queensland solar feed-in tariffs and the merit-order effect: economic benefit, or regressive taxation and wealth transfers?," *Economic Analysis and Policy*, vol. 42, no. 3, p. 257, 2012.

[28] D. Marshman, M. Brear, M. Jeppesen, and B. Ring, "Performance of wholesale electricity markets with high wind penetration," *Energy Economics*, p. 104803, 2020.

[29] J. Riesz, I. MacGill, and J. Gilmore, "Examining the viability of energy-only markets with high renewable penetrations," in *2014 IEEE PES General Meeting—Conference & Exposition*, pp. 1–5, IEEE, 2014.

[30] I. J. Pérez-Arriaga and C. Meseguer, "Wholesale marginal prices in competitive generation markets," *IEEE Transactions on Power Systems*, vol. 12, no. 2, pp. 710–717, 1997.

[31] M. Caramanis, "Investment decisions and long-term planning under electricity spot pricing," *IEEE Transactions on Power Apparatus and Systems*, no. 12, pp. 4640–4648, 1982.

[32] M. C. Caramanis, R. E. Bohn, and F. C. Schweppe, "Optimal spot pricing: Practice and theory," *IEEE Transactions on Power Apparatus and Systems*, no. 9, pp. 3234–3245, 1982.

[33] R. P. O'Neill, P. M. Sotkiewicz, B. F. Hobbs, M. H. Rothkopf, and W. R. Stewart Jr, "Efficient market-clearing prices in markets with nonconvexities," *European journal of operational research*, vol. 164, no. 1, pp. 269–285, 2005.

[34] W. W. Hogan and B. J. Ring, "On minimum-uplift pricing for electricity markets," *Electricity Policy Group*, pp. 1–30, 2003.

[35] F. Ueckerdt, L. Hirth, G. Luderer, and O. Edenhofer, "System LCOE: What are the costs of variable renewables?," *Energy*, vol. 63, pp. 61–75, 2013.

[36] F. J. de Sisternes, M. D. Webster, and I. J. Pérez-Arriaga, "The impact of bidding rules on electricity markets with intermittent renewables," *IEEE Transactions on Power Systems*, vol. 30, no. 3, pp. 1603–1613, 2015.

[37] Bureau of Resources and Energy Economics, "Australian Energy Technology Assessment," 2012. Available http://www.bree.gov.au/publications/australian-energy-technology-assessments.

[38] W. J. Cole and A. Frazier, "Cost projections for utility-scale battery storage," 2019. Available National Renewable Energy Lab (NREL). Available https://www.nrel.gov/docs/fy19osti/73222.pdf.

[39] J. A. Hayward and P. W. Graham, "Electricity generation technology cost projections," December 2017. Commonwealth Scientific and Industrial Research Organisation (CSIRO). Available https://publications.csiro.au/rpr/download?pid=csiro:EP178771&dsid=DS2.

[40] D. Marshman, *Performance of electricity markets & power plant investments in the transition to a low-carbon power system*. PhD thesis, 2018.

[41] B. S. Palmintier and M. D. Webster, "Heterogeneous unit clustering for efficient operational flexibility modeling," *IEEE Transactions on Power Systems*, vol. 29, no. 3, pp. 1089–1098, 2013.

[42] P. Kundur, N. J. Balu, and M. G. Lauby, *Power system stability and control*, vol. 7. McGraw-hill New York, 1994.

[43] Australian Energy Market Commission, "National Electricity Market Rules Version 150," September 2020. Available https://www.aemc.gov.au/sites/default/files/2020-09/NER%20v150%20full_0.pdf.

[44] Commission for Regulation of Utiltiies, "Rate of Change of Frequency Project Quarterly Report for Q1 & Q2 2019," July 2019. Available https://www.aemc.gov.au/sites/default/files/2020-09/NER%20v150%20full_0.pdf.

[45] GAMS Development Corporation, "General Algebraic Modeling System (GAMS) Release 24.1.3," 2013. Available http://www.gams.com/.

[46] P. Simshauser, "On intermittent renewable generation & the stability of Australia's National Electricity Market," *Energy Economics*, vol. 72, pp. 1–19, 2018.